RSC Advances

PAPER

View Article Online
View Journal | View Issue

Cite this: *RSC Adv.*, 2021, **11**, 23892

Enhancing the reinforcing efficiency in CNT nanocomposites *via* the development of pyrene-based active dispersants†

Xinyi Yin,‡[ab] Qiang Li,‡[bc] Haishui Wang,[a] Wengang Yang,[b] Xi Zhou,*[b] Han Zhang *[d] and Weibang Lyu *[be]

Received 12th May 2021
Accepted 23rd June 2021

DOI: 10.1039/d1ra03711k

rsc.li/rsc-advances

Various preforms of carbon nanotubes (CNTs), such as fibers, yarns, or buckypapers (BP), have been developed over the last few years in order to fabricate advanced nanocomposites containing a high volume fraction of the reinforcing phase. However, a homogeneous dispersion and an even isolation of CNTs during the fabrication process of many preforms such as BP is often challenging, while the poor interaction between CNTs and the matrix also limits the final performance of the nanocomposites. Herein, a new route to overcome these two challenges simultaneously has been demonstrated based on an active dispersant (noted as Py-PEI) developed through the quaternization reaction of pyrene derivatives (Py-Br) and polyethylenimine (PEI). The existence of pyrene groups leads to the formation of π–π stacking with CNTs, successfully hindering the re-aggregation of dispersed CNTs. Meanwhile, the amine groups of Py-PEI can establish covalent bonds with epoxy, leading to an enhanced load transfer efficiency between CNTs and epoxy in the composites. Systematic characterization of both fabricated BP and BP-reinforced nanocomposites have been performed, with significantly enhanced CNT dispersion stability in water together with improved mechanical performance of the as-obtained BP/epoxy nanocomposites. This study provides a new strategy in fabricating high performance nanocomposites with the ease of nanofiller dispersion and enhanced reinforcing efficiency.

1. Introduction

Since the discovery of carbon nanotubes (CNTs) in 1991,[1] a great amount of effort has been dedicated in developing lightweight, high-performance and multi-functional composites by utilizing the excellent mechanical strength, electrical and thermal properties of CNTs.[2,3] Nevertheless, two features of CNTs often limit their strengthening efficiency in nano-reinforced composites: (i) high level of entanglement of CNTs due to their high aspect ratios, high surface areas and inter-tube van der Waals interactions, which often results in agglomerations and poor dispersion/distribution in the matrix; (ii) the inert nature of the pristine CNT surfaces, causing poor compatibility or weak interfacial interaction with the matrix; hence, a limited reinforcing efficiency in subsequent composites.

Among many CNT assemblies developed during the last two decades to overcome the dispersion and agglomeration issues, buckypaper (BP) consisting of pure CNTs in the form of a thin film with a thickness of around few hundred microns provides an easy solution in handling and subsequent nanocomposite fabrication.[4–6] Both dry method[7] and wet method[8] have been developed in making BPs. However, the wet method, where BPs are made by filtrating CNT solutions through porous membranes, is more widely used owing to its simplicity and easy operation, and the product structure can be well predicted and controlled.[9]

A uniform CNT dispersion is essential and of great necessity in making high-performance BP films *via* wet method. Thus, the selection of appropriate dispersant and dispersing media to prepare the CNT suspension becomes a crucial step of the process. As most dispersing media employed are organic solvents, such as *N*,*N*-dimethylformamide (DMF) and acids, deionized (DI) water is becoming one of the most desired options owing to its environment-friendly nature, although the hydrophobic nature of CNTs often hinders the dispersion

[a]*School of Chemistry and Chemical Engineering, South China University of Technology, Guangzhou 510641, China*

[b]*Innovation Center for Advanced Nanocomposites, Suzhou Institute of Nano-Tech and Nano-Bionics, Chinese Academy of Sciences, Suzhou 215123, China. E-mail: wblv2013@sinano.ac.cn; xzhou2020@sinano.ac.cn*

[c]*School of Nano Science and Technology Institute, University of Science and Technology of China, Suzhou 215123, China*

[d]*School of Engineering and Materials Science, Queen Mary University of London, London E1 4NS, UK. E-mail: han.zhang@qmul.ac.uk*

[e]*Division of Nanomaterials, Jiangxi Key Lab of Carbonene Materials, Suzhou Institute of Nano-Tech and Nano-Bionics, Chinese Academy of Sciences, Nanchang 330200, Jiangxi, China*

† Electronic supplementary information (ESI) available. See DOI: 10.1039/d1ra03711k

‡ Co-first author.

process in DI. Many surfactants, such as sodium dodecylbenzene sulfonate (SDBS), polyvinylpyridone (PVP), and sodium cholate (SC) have been used as dispersants to facilitate the CNT dispersion. However, it is worth noting that these employed surfactants usually remained on CNT surfaces after dispersion and become contaminations. Hence, they weaken the interface load transfer, requiring an additional removal process such as acid treating,[10,11] annealing[12,13] and soaking or washing.[14,15] Clearly, it is essential and of great important to have a dispersant that stabilizes the CNT dispersion without the aforementioned side effects.

It is well known that the existence of a thin layer of sizing agents on the surface of advanced fibers (*e.g.*, carbon fibers, glass fibers) can provide the bonding between the reinforcing fibers and matrix with an enhanced load transfer. Introducing chemical groups onto the CNT surfaces for a similar purpose – to establish a stronger interaction between the CNTs and matrix – has been proven as an efficient method in enhancing the final performance of the CNT composites. Similar to fiber sizing, the ideal active dispersant for CNTs should meet the following two requirements: forming the non-covalent bonds with CNT surfaces during the dispersion stage, and the covalent bonds with matrix materials during the subsequent manufacturing stage. The former reserves the conjugated atomistic structure of CNTs and prohibits the dispersed CNTs from re-aggregation, while the latter enhances the load transfer efficiency between the matrix and CNTs in the composites.

Over the last few years, many efforts have been made to design and synthesize active dispersants for CNTs. Chen *et al.* reported a non-covalent modification strategy that utilized tannic acid (TA) and polyethylenimine to aid the CNT dispersion, and to improve the interfacial interaction between multi-walled carbon nanotubes (MWCNTs) and the epoxy matrix based on the reaction between the amine group on the surface of MWCNTs and epoxy resins.[16] Gu *et al.* developed a dispersant based on polystyrene (PS) grafted with epichlorohydrin, which could interact with MWCNT *via* π–π stacking and covalently bond with the epoxy resin matrix *via* the epoxy–amine reaction, obtaining increased tensile strength and bending strength by 37.6% and 34.4%, respectively.[17] In another study, Park *et al.* found that the π–π interaction between phenyl glycidyl ether (PGE) and MWCNT could enhance the dispersion of MWCNT. Meanwhile, the epoxy functional groups contained in PGE can improve the interfacial properties through the covalent bond with the polyamide-6 matrix.[18] It was also found that compared with the molecules containing single aromatic rings, such as the aforementioned TA, PS, and PGE, pyrene derivatives that contain four or more aromatic rings have been proved to form much enhanced interactions with CNTs.[19]

In this work, an environmental-friendly water-based suspension with stable CNT dispersion alongside improved interfacial bonding has been achieved for enhanced reinforcing efficiency in the fabricated nanocomposites. A new active dispersant has been developed based on the water-soluble branched polymer polyethyleneimine (PEI) containing sufficient reactive amine groups (primary, secondary and tertiary) *via* quaternization reaction between 1-(bromoacetyl) pyrene (Py-Br) and PEI. A stable CNT dispersion in water has been successfully achieved for an extended period of time (over one month) owing to the formation of π–π interactions between the pyrene groups and CNTs. In addition, with the established covalent bonds between the amine groups and epoxy matrix, CNT composites with improved mechanical properties have been achieved. This work provides a new route to overcome the low reinforcing efficiency in CNT nanocomposites with an environmentally sustainable water suspension consisting of a stable CNT dispersion, benefiting the field of nanocomposites with the easiness of sustainable fabrication without organic solvents for high performance applications.

2. Experimental

2.1 Raw materials

Single-walled carbon nanotubes (SWCNTs) were provided by Nanjing JCNano Technology Co., Ltd. The diameter and length of these CNTs were about 1–2 nm and 15–20 μm, respectively, according to the datasheet provided. 1-(Bromoacetyl)pyrene (Py-Br, 97%) was purchased from Merck Corp. Polyethyleneimine (PEI) with an average molecular weight of 600 g mol^{-1} was purchased from Aladdin Reagent Corp, Shanghai, China. Sodium dodecyl benzene sulfonate (SDBS, AR), *N*,*N*-dimethylformamide (DMF, AR), tetrahydrofuran (THF, AR) and acetone were purchased from Sinopharm Chemical Reagent Co., Ltd. Epoxy resin DER332 was purchased from Dow Chemical Co. The amine curing agents, 4,4′-methylenedianiline (DDM) and 2-ethyl-4-methylimidazole (2E4MZ), were formulated in the laboratory prior to use. All chemicals and solvents were used as received and without further purification. Deionized (DI) water was generated with a Milli-Q integral pure and ultrapure water purification system.

2.2 Preparation of materials

2.2.1 Preparation of the active dispersant. To make the active dispersant, 97 mg Py-Br was dissolved in 6 mL DMF and 60 mg PEI was dissolved in 10 mL DMF beforehand. Then, the yellowish Py-Br solution was added dropwise into the prepared PEI solution, where the color of the PEI solution changed from colorless to yellowish, and then quickly went to wine red. The mixtures were stirred for 12 hours at room temperature, and then precipitated in 100 mL THF to remove the unreacted Py-Br. The precipitates were collected *via* centrifuge (7000 rpm, 15 min), and subsequently dissolved in DMF and precipitated in THF again. The dissolve–precipitate–centrifuge procedure was repeated several times until no obvious color change was observed in the liquid supernatant. The precipitates were then dried overnight in vacuum at 100 °C. The final product in brownish yellow was obtained and labeled as Py-PEI, and the yield was about 60 wt%.

2.2.2 Preparation of the CNT dispersions. 36 mg Py-PEI and 36 mg SDBS were individually dissolved in 120 mL DI water before the addition of 12 mg of CNTs into each solution. Both mixtures were then individually homogenized by using a high-pressure jet-milling homogenizer (20 MPa, AH-BASIC 2,

ATS Engineering Limited) for 30 min to obtain CNT dispersions, which were denoted as Py-PEI@CNT and SDBS@CNT, respectively. For comparison, 12 mg CNTs were added into 120 mL DI water to prepare pure CNT dispersions under the same conditions, and the obtained suspension was denoted as p-CNT.

2.2.3 Preparation of the BP film and BP-based composite film. The above dispersions were filtered through a cellulose acetate membrane with a pore size of 0.2 μm and diameter of 47 mm, and then rinsed with DI water several times. The obtained BP films, labeled as Py-PEI@BP, SDBS@BP and p-BP, were dried for 24 hours at room temperature, and then carefully peeled from the filter membrane. The epoxy DER332 and curing agent (epoxy/curing agent = 100 : 27 by weight) were dissolved in acetone with a resin content of 8 wt%. The BP films were soaked in the above solution for 2 hours at 50 °C, and then dried in a vacuum for 0.5 h at 35 °C to remove acetone. Between 2 to 4 pieces of infiltrated BP films were stacked together to provide an appropriate thickness, and then cured by hot pressing at 20 MPa, 100 °C for 1 hour and 140 °C for 4 hours. The obtained composite films, which were around 20 μm thick, were labeled as Py-PEI@BP/(Epoxy-8), SDBS@BP/(Epoxy-8) and p-BP/(Epoxy-8). To study the effect of the resin content on the composite properties, solutions containing 5 wt%, and 10 wt% resin were also prepared, and the resulting Py-PEI@BP based composites were labeled Py-PEI@BP/(Epoxy-5) and Py-PEI@BP/(Epoxy-10) accordingly.

2.3 Characterization

The synthesized dispersants were characterized by Ultraviolet-visible and near-infrared spectroscopy (UV-Vis-NIR, Cary 5000, Agilent) from 200 nm to 500 nm and Fourier Transform infrared spectroscopy (FT-IR, Nicolet 6700, Thermo Scientific, USA) within the scan range of 4000–500 cm^{-1}. Functionalization of CNTs was also analyzed by FT-IR. The ratio of I_D/I_G was obtained using a Raman microscope (LabRAM ARAMIS Horiba Jobin Yvon) with a 532 nm diode pumped solid-state laser. X-ray photoelectron spectroscopy (XPS, ESCALAB Xi^+, Thermo Scientific) was performed to observe the chemical structure of BP. The thermal behaviors of the samples and the content of epoxy and dispersant within the composites were examined by thermogravimetry (TGA, TG 209 F1 Libra, NETZSCH) under N_2, with the temperature increasing from 30 °C to 600 °C at a heating rate of 10 °C min^{-1}. The curing reaction between the epoxy and dispersant was determined by differential scanning calorimetry (DSC, 200 F3 Maia, NETZSCH) from 30 °C to 200 °C with a heating rate of 10 °C min^{-1} under N_2. The microstructures of the BP films were observed using a scanning electron microscope (SEM, S4800, Hitachi, Japan). The morphologies of the CNTs were characterized by transmission electron microscopy (TEM, Tecnai G2F20 S-Twin, FEI, USA) operated at 200 kV. The mechanical properties, including the tensile strength, modulus and strain to failure of the BP films were characterized using a tensile testing machine (Instron 3365, Instron Inc. USA) equipped with a 10 N load cell. Specimens were cut into pieces of 1 mm in width and 20 mm in length. The gauge length was 10 mm and the crosshead displacement speed was 0.5 mm min^{-1}. At least five specimens were tested for each kind of sample with average values reported in the results section.

3. Results and discussion

3.1 Chemical structures of the active dispersant Py-PEI

As schematically illustrated in Fig. 1a, Py-PEI was synthesized by the quaternization reaction between Py-Br and PEI. FTIR was used to determine the chemical bonds and structures of the synthesized specimens, with the typical spectra of PEI, Py-Br presented alongside with Py-PEI. As shown in Fig. 2a, the FTIR analysis discloses the presence of the absorption peaks at 2871 cm^{-1}, 1660 cm^{-1} and 852 cm^{-1}, assigned to the quaternary ammonium salt, carbonyl group adjacent to the pyrene group, and C–H in the pyrene ring, respectively.[20] This indicates the successful introduction of the pyrene group into PEI *via* quaternization. In addition, the appearance of broad and strong peaks between 3500–3100 cm^{-1} confirmed the existence of abundant amine groups (–NH_2 and –NH–) in Py-PEI, which would benefit the subsequent interaction with epoxy resins. UV-Vis-NIR diagnosis (Fig. 2b) clearly showed the characteristic absorption K band of the pyrene group between 310–420 nm due to the π–π* transition in the spectrum of Py-PEI, further confirming the presence of the pyrene group in Py-PEI.[21]

3.2 Dispersion of CNTs aided by Py-PEI

The effect of Py-PEI on the CNT dispersion has been characterized and presented in Fig. 3, with the optical images of the dispersed CNT suspensions after 10 minutes (Fig. 3a) and 1 month (Fig. 3b). After 0.05 mg mL^{-1} CNTs were dispersed in deionized water *via* high-pressure jet-milling homogenizer for 30 min, the pure CNT suspension (p-CNT) showed very clear precipitation after 10 min only, while the Py-PEI@CNT and SDBS@CNT suspensions remained homogeneous without

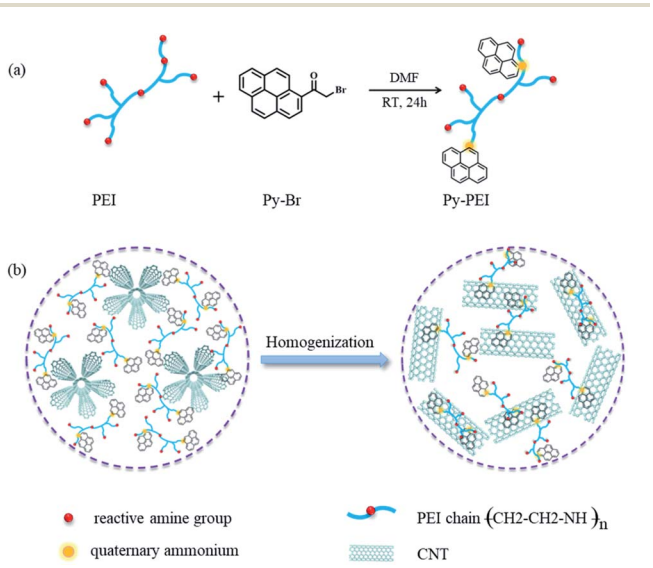

Fig. 1 Schematic illustrations of (a) the preparation process of the active dispersant Py-PEI; and (b) the mechanism of the Py-PEI facilitated CNT dispersion without re-aggregation after dispersion.

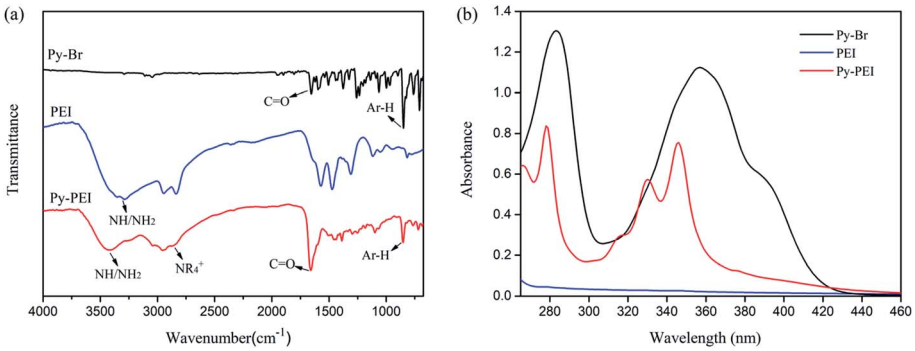

Fig. 2 (a) IR spectra of Py-Br, PEI, and synthesized Py-PEI, indicating the presence of the pyrene group in PEI after quaternization; and (b) UV-Vis-NIR spectra of PEI, Py-Br and synthesized Py-PEI, with a clear trace of the characteristic K band from the pyrene group at the 310–420 nm range.

obvious precipitation. After an extended period of time (one month) at room temperature, flocculation took place in the SDBS@CNT suspension (Fig. 3b), while the Py-PEI@CNT suspension was still showing a very stable dispersion, indicating the efficiency of Py-PEI in facilitating a stable CNT dispersion in DI water.

The morphologies of both pristine and Py-PEI-coated CNTs were examined and analyzed through TEM. As shown in Fig. 3c, the pristine CNTs sample presented relatively smooth surfaces, while the Py-PEI modified CNT samples showed evidence of the Py-PEI molecules wrapping around the CNTs (Fig. 3d), serving as a spatial barrier to prevent the re-aggregation of CNTs in the solution.

As schematically illustrated in Fig. 1b, the improved CNT dispersion after Py-PEI modification can be attributed to the pyrene groups anchored on the surface of the isolated CNTs, forming π–π stacking and providing barriers between CNTs to prevent them from re-aggregation.

3.3 Structure and morphology of the Py-PEI functionalized BP film

The chemical structure of BP films was analyzed by FT-IR spectroscopy, as shown in Fig. 4a. For the pristine CNTs, no absorption peak was observed, indicating that the surface of the unmodified CNTs is relatively clean. For Py-PEI@BP, however, several absorption peaks can be clearly identified. These strong peaks located between 3500–3100 cm^{-1}, at 1635 cm^{-1} and at 852 cm^{-1} mainly originated from the amine groups ($-NH_2$ and –NH–), carbonyl group and C–H in the pyrene ring of Py-PEI, confirming the presence of Py-PEI on the CNT surfaces.

Raman spectroscopy was used to analyze the effect of functionalization on the intrinsic structure of CNTs. The relative intensity (I_D/I_G) between the D-band and G-band is a good parameter to evaluate the structural defects of CNTs.[16] The intensity ratios of the D-band and G-band of the p-BP film and Py-PEI@BP film were 0.0235 and 0.0244, respectively, as shown

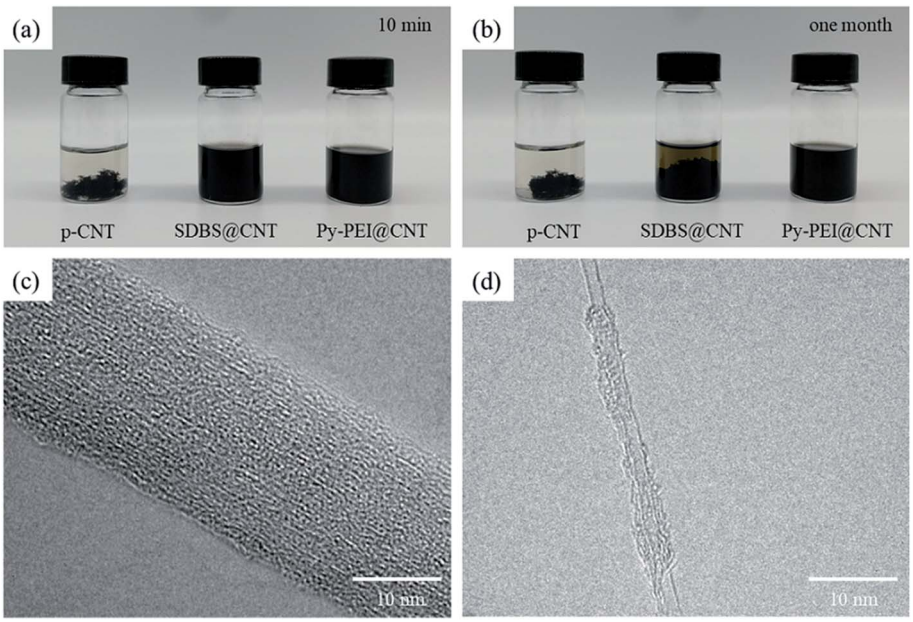

Fig. 3 Digital pictures of the CNTs suspensions (0.05 mg mL^{-1}) after (a) 10 minutes and (b) one month, as well as TEM images of CNTs in DI water (c) before and (d) after Py-PEI treatment.

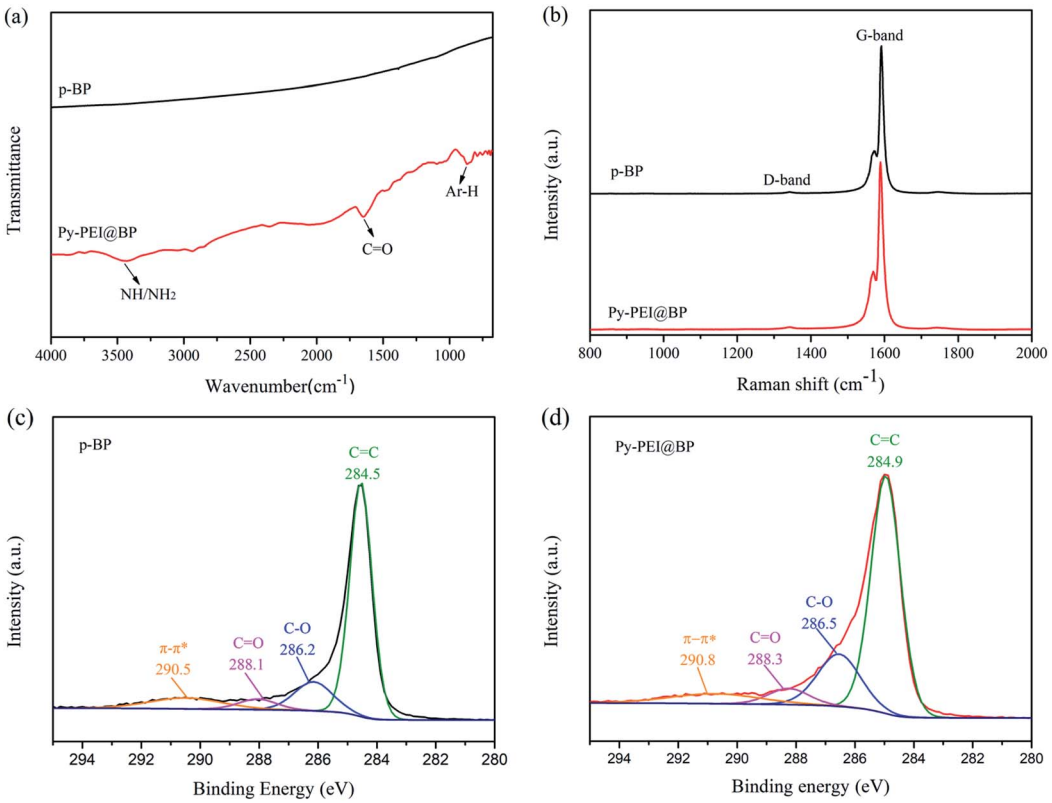

Fig. 4 (a) FT-IR spectra showing clear evidence of Py-PEI at the surface of the treated CNTs; and (b) Raman spectra of the p-BP film and Py-PEI@BP film; XPS C1s spectra of (c) the p-BP film, (d) Py-PEI@BP film.

in Fig. 4b. This indicates that the non-covalent functionalization process by Py-PEI has successfully preserved the crystal structure of CNTs without any obvious damage. According to a previous report, the G-band shifted to a higher frequency (blue shift) after p-doping and to lower frequency (red shift) after n-doping.[22] Compared to the p-BP film, the G band of the Py-PEI@BP film was slightly red-shifted by about 2 cm^{-1} (from 1591 cm^{-1} to 1589 cm^{-1}), indicating the existence of an electron transfer from Py-PEI to CNTs.[23]

XPS was utilized to examine the interaction between Py-PEI and CNTs. As shown in Fig. 4c and d, the main C1s peak of CNTs had changed in position and in intensity after Py-PEI treatment. The shift of the peak position was used to characterize the charge transfer between Py-PEI and CNTs.[23] The main peak of C1s of the p-BP film appeared at 284.5 eV, which was regarded as the sp^2 carbon. The main C1s peak of the Py-PEI@BP film was up-shifted by 0.4 eV compared to the p-BP film, indicating the electron transfer from Py-PEI to CNTs, which is consistent with the Raman data observed. The increase of the C=C signal intensity is mainly attributed to the graphene-like structure of the pyrene group in Py-PEI.[24]

The π–π* transition was observed in the spectrum of both p-BP films (290.5 eV) and Py-PEI@BP films (290.8 eV). In the p-BP film, the π–π* transition was caused by inter-tube interaction of CNTs, which exist in the form of large size bundles. While in Py-PEI@BP film, the π–π* transition in this film originated not only from the interaction between CNTs within a bundle, but also from the interaction between pyrene groups and CNTs. The peak position of the π–π* transition in the Py-PEI@BP film was up-shifted by 0.3 eV, indicating a stronger electron donor effect. This discloses the strong interaction between Py-PEI and CNTs *via* π–π stacking, and confirms the successful attachment of Py-PEI onto CNTs.

As shown in Fig. 5, although all BP films were composed of a CNT bundle network with porous structures, most of the bundles in the Py-PEI@BP film were below 50 nm in diameter (Fig. 5c), which is smaller than that of the SDBS@BP film (Fig. 5b) and far smaller than that of the pristine BP film (Fig. 5a). The presence of a larger amount of thin CNT bundles in the Py-PEI@BP film indicates that Py-PEI has excellent performance in stabilizing the CNT suspension during the dispersion/filtration processing. Compared with one of the widely used surfactants (SDBS), the pyrene-decorated polymers, anchored around the surface of CNTs *via* π–π stacking, effectively decreased the tendency of re-aggregation of CNTs. In addition, although the Py-PEI@BP films were shown to be more compact than pristine BP, the presence of fine porosity with pore sizes of around 50–300 nm allowed for sufficient cavities for the epoxy resin to impregnate the CNT films during the manufacturing processes.[15]

3.4 Mechanical performance analyses

3.4.1 Py-PEI, CNTs and epoxy contents in the fabricated composite films. TGA was performed to determine the content

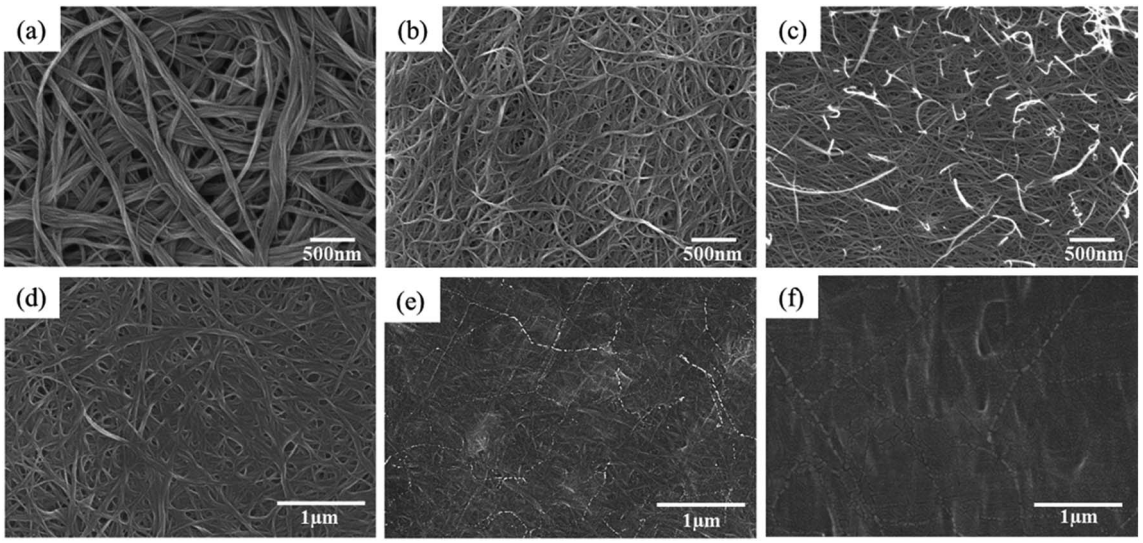

Fig. 5 SEM images of the (a) p-BP film, (b) SDBS@BP film, and (c) Py-PEI@BP film show much thinner and separated CNT bundles owing to the enhanced stable CNT dispersion, (d) Py-PEI@BP/(Epoxy-5), (e) Py-PEI@BP/(Epoxy-8) and (f) Py-PEI@BP/(Epoxy-10).

of Py-PEI and CNTs in the Py-PEI@BP film and Py-PEI, CNTs, as well as the epoxy matrix in the composite samples. About 5 mg of the sample was used for TGA analysis. At least three samples were tested for each material, which showed a relatively constant distribution of ingredients. TGA curves of different samples and their residual fraction were obtained (Fig. S1†) after these samples were heated to 600 °C. The content of each component in the Py-PEI@BP film and composite samples were then calculated accordingly (see ESI† for details) and summarized in Table 1.

It can be found that the Py-PEI@BP film is composed of approx. 34 wt% Py-PEI and 66 wt% CNTs. The relatively high amount of dispersant left in the BP film implies good interaction between the active dispersant and CNTs. It is worth noting that the original ratio of Py-PEI and CNTs was 3, while after filtration, the ratio was reduced to about 0.5. This means that a certain amount of Py-PEI materials did not form intimate interactions with CNTs, and were removed during the filtration processing. For composite samples, the content of CNTs was in the range of 34 wt%–43 wt%, which is a relatively high amount as reinforcement in the composites, especially considering the random in-plane distribution nature of the current nanocomposites films. The relative amount of Py-PEI was around 18 wt%–22 wt%, which provides adequate amine groups to cross-link with the epoxy matrix during the curing process.

Table 1 The contents of Py-PEI, CNTs and epoxy in the composite films

		Content of each component (wt%)		
Sample	Residual mass (%)	Py-PEI	CNTs	EP
BP	97.5	—	97.5	—
Py-PEI	17.1	17.1	—	—
Py-PEI@BP	70.2	34.0	66.0	—
Py-PEI@BP/(Epoxy-5)	46.1	22.3	43.4	34.3
Py-PEI@BP/(Epoxy-8)	39.5	19.1	37.1	43.8
Py-PEI@BP/(Epoxy-10)	36.8	17.8	34.6	47.6

3.4.2 Mechanical properties. The representative stress–strain curves of different BP films were shown in Fig. 6a and the overall mechanical properties were summarized in Fig. 6b. For pure BP films without any resins, CNTs were not well dispersed or exfoliated in the dispersion, connecting to each other only through inter-tube van der Waals forces thus resulted in very low tensile strength and modulus. However, using Py-PEI to facilitate the dispersion, the modified film already demonstrated a better mechanical performance without any resins, attributed to the improved quality of the dispersion and sufficient separation of the CNT bundles, as observed from morphological studies (Fig. 5c).

The introduction of epoxy resins plays an important role in impregnating and binding CNTs to transfer the external stress to CNTs *via* interfacial load transfer. However, the amount of resin should be carefully controlled to ensure decent bonding, yet sufficiently high content of reinforcing CNTs. By impregnating the Py-PEI@BP film in 5 wt%, 8 wt% and 10 wt% epoxy resin solutions, CNT composites, named Py-PEI@BP/(Epoxy-5), Py-PEI@BP/(Epoxy-8), and Py-PEI@BP/(Epoxy-10) accordingly, were obtained. As shown in Table 1, the effective CNT concentrations of these three composites are 43.4 wt%, 37.1 wt%, and 34.6 wt%, respectively.

As shown in Fig. 6a, the tensile strength and modulus of the composites made through impregnating the BP with a lower concentration of 5 wt% were about 135.1 MPa and 10.8 GPa, respectively. This moderate reinforcing efficiency can be attributed to the existence of voids, as observed from SEM images (Fig. 5d). With the increased amount of epoxy EP content of 8 wt% in the impregnation solution (effectively 37.1 wt% CNTs), much higher tensile strength and modulus of

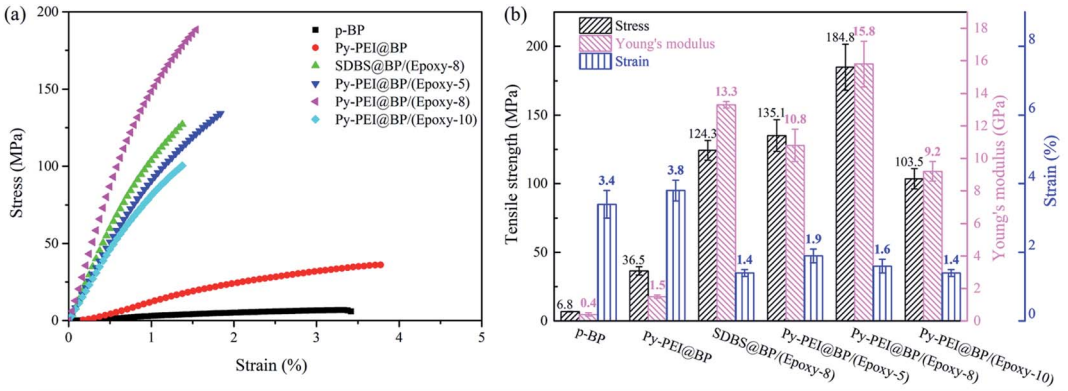

Fig. 6 Mechanical properties of BP and their based composites: (a) the representative stress–strain curves, (b) mechanical properties' bar chart of different films.

184.8 MPa and 15.8 GPa were obtained, respectively. This excellent mechanical performance of the nanocomposites is in good agreement with their compact and uniform microstructure, as revealed from Fig. 5e. When further increasing the EP amount (effectively with 34.6 wt% CNTs), a resin rich layer was found on the surface of the composite films in Fig. 5f, resulting in reduced mechanical properties of 103.5 MPa in tensile strength and 9.2 GPa in modulus from previous specimens. These enhanced mechanical properties are also compared with other widely used surfactant (SDBS@BP/(Epoxy-8)) at the same concentration of the Py-PEI decorated specimens, as shown in Fig. 6a. As expected, higher values in both stiffness (15.8 GPa to 13.3 GPa) and strength (184.8 MPa to 124.3 MPa) can be found from the Py-PEI@BP/(Epoxy-8) film compared with SDBS@BP/(Epoxy-8) films, owing to the enhanced interfacial interaction between the Py-PEI molecules and epoxy resins, where the residual SDBS molecules could not form strong covalent bonds with the epoxy matrix.

The excellent reinforcing efficiency and improved stiffness and strength of the CNT nanocomposites are attributed to two main aspects: (i) homogeneous dispersion and stable suspension with very well isolated CNTs owing to the active dispersant Py-PEI, leading to increased surface areas of CNTs exposed for subsequent interaction with resins; (ii) promoted stress transfer from the resin matrix to CNTs owing to the successful introduction of amine groups from the Py-PEI molecules, providing covalent bonding with the epoxy resins during the cross-linking process; hence, enhanced interactions between CNTs and epoxy resins. The cross-link reaction between Py-PEI and epoxy was verified by DSC analysis (Fig. S3†), where a curing exothermic peak starting from 125 °C in the Py-PEI/epoxy curve can be found.

Within p-BP, neighboring CNTs (either parallel aligned or crossed) interact with each other through weak van der Waal interactions. Upon stretching, CNTs can slide with each other easily. After the impregnation of the epoxy resin, CNTs were coated by resin materials. On the one hand, this enhanced the load transfer between CNTs, while on the other hand, it restricted the inter-tube sliding. Thus, the failure strain of the CNT composites is lower than that of p-BP. Similar phenomena have also been reported in previous studies, such as ref. 14 and 25.

Fig. 7 compared the tensile strength and modulus of the BP-based CNT/epoxy films reported in the literature.[14,25–31] It can be seen that the tensile strength of the composite films developed in the current study are among one of the highest reported values for the modulus, further confirming the reinforcing efficiency of the current "sizing" layer on the surface of CNTs in the epoxy nanocomposites.

4. Concluding remarks and discussions

In this study, we developed a universal method to design an active dispersant for CNTs. We solved not only the well-acknowledged re-agglomeration issues in the CNT dispersion, but also the interfacial load transfer between the CNT reinforcement and epoxy resins in the nanocomposites. A new "active dispersant" Py-PEI was successfully synthesized *via* quaternization reaction between 1-(bromoacetyl) pyrene (Py-Br) and polyethyleneimine (PEI), serving as a "sizing" layer for

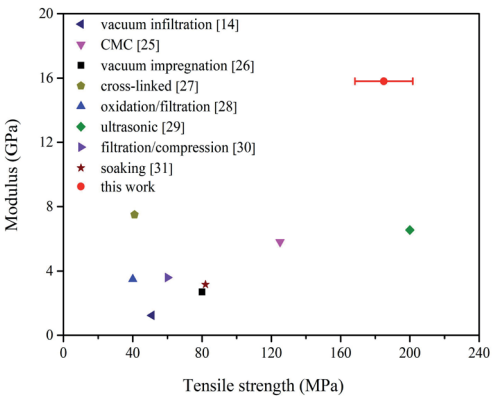

Fig. 7 Comparison of the mechanical properties of wet-processed BP/epoxy nanocomposite films with various treatments, confirming the excellent reinforcing efficiency introduced from the effective dispersion and enhanced interfacial load transfer in the current system.

CNTs similar to the commercial microsized reinforcing fibers. A very stable CNT dispersion has been achieved in a water suspension without any sign of re-agglomeration even after a prolonged period of time, which can provide enhanced processability for the subsequent nanocomposite, especially with an environmentally friendly medium, such as water.

Based on the developed active dispersant, high quality BPs and BP-based CNT composites have been fabricated and systematically characterized, in order to examine the interfacial load transfer based on the Py-PEI sizing layer and subsequent performance. Excellent mechanical performance owing to the enhanced reinforcing efficiency at the interfacial areas have been obtained. The modulus of 15.8 GPa at 37.1 wt% CNT loadings is among one of the highest reported values in the BP-based nanocomposites, attributed to the covalent bonds formed between Py-PEI and epoxy resins. It is also worth noting that the presented strategy in developing an active dispersant can be tuned for other resin systems, offering great potential in a wide range of resin systems.

It is worth mentioning that the strength of the composite films prepared by dry method can often reach over 2 GPa.[32,33] It is well recognized that besides the factor of interfacial load transfer, the length and alignment of CNTs are other two key factors determining the mechanical performance of the CNT composite. In the CNT films prepared through the dry methods, either drawing from a spinnable array or directly synthesized using the floating catalyst CVD method, CNTs are always in the order of hundreds of micrometers. However, CNTs used in the current study are far shorter, which is only around ten micrometers. Moreover, CNTs in the current composites were almost randomly distributed. Thus, using longer CNTs and increasing the alignment of CNTs should be the focus of preparing high-performance BP-based composites in the future.

Author contributions

Xinyi Yin: methodology, formal analysis, validation, data curation, investigation, writing – original draft. Qiang Li: validation, formal analysis, data curation, writing-original draft. Haishui Wang: funding acquisition, writing-review & editing, supervision. Wengang Yang: methodology, validation, formal analysis, data curation. Han Zhang: conceptualization, writing-review & editing, supervision. Weibang Lu: conceptualization, supervision, project administration, funding acquisition, writing-review & editing.

Conflicts of interest

The authors declare that they have no known competing financial interests or personal relationships that could have appeared to influence the work reported in this paper.

Acknowledgements

The authors acknowledge the support from the National Key Research and Development Program of China (2016YFA0203301) and the Foundation of National Natural Science Foundation of China (No. 21773072).

Notes and references

1 S. Iijima, *Nature*, 1991, **354**, 56–58.
2 M. F. L. De Volder, S. H. Tawfick, R. H. Baughman and A. J. Hart, *Science*, 2013, **339**, 535–539.
3 I. A. Kinloch, J. Suhr, J. Lou, R. J. Young and P. M. Ajayan, *Science*, 2018, **362**, 547–553.
4 A. Kausar, H. Ilyas and M. Siddiq, *Polym.-Plast. Technol. Eng.*, 2017, **56**, 1780–1800.
5 M. T. Byrne and Y. K. Gun'ko, *Adv. Mater.*, 2010, **22**, 1672–1688.
6 J. Liu, A. G. Rinzler, H. J. Dai, J. H. Hafner, R. K. Bradley, P. J. Boul, A. Lu, T. Iverson, K. Shelimov, C. B. Huffman, F. Rodriguez-Macias, Y. S. Shon, T. R. Lee, D. T. Colbert and R. E. Smalley, *Science*, 1998, **280**, 1253–1256.
7 H. M. Cheng, F. Li, G. Su, H. Y. Pan, L. L. He, X. Sun and M. S. Dresselhaus, *Appl. Phys. Lett.*, 1998, **72**, 3282–3284.
8 S. Qu, Y. Dai and D. Zhang, *Funct. Compos. Struct.*, 2020, **2**, 2002–2037.
9 Q. Xia, Z. Zhang, Y. Liu and J. Leng, *Composites, Part B*, 2020, **199**, 108231.
10 H. Z. Geng, K. K. Kim, K. P. So, Y. S. Lee, Y. Chang and Y. H. Lee, *J. Am. Chem. Soc.*, 2007, **129**, 7758–7759.
11 Q. Liu, T. Fujigaya, H.-M. Cheng and N. Nakashima, *J. Am. Chem. Soc.*, 2010, **132**, 16581–16586.
12 X. Jiang, W. Gong, S. Qu, D. Wang, T. Liu, Q. Li, G. Zhou and W. Lu, *Carbon*, 2020, **169**, 17–24.
13 Y.-A. Leu, M.-H. Yeh, L.-Y. Lin, T.-J. Li, L.-Y. Chang, S.-Y. Shen, Y.-S. Li, G.-L. Chen, W.-H. Chiang, J.-J. Lin and K.-C. Ho, *ACS Sustainable Chem. Eng.*, 2017, **5**, 537–546.
14 S. C. Her and W. C. Hsu, *Nanomaterials*, 2020, **10**, 2258–2268.
15 Z. Wang, Z. Y. Liang, B. Wang, C. Zhang and L. Kramer, *Composites, Part A*, 2004, **35**, 1225–1232.
16 Y. Chen, W. Wei, Y. Zhu, J. Luo and X. Liu, *Compos. Sci. Technol.*, 2019, **170**, 25–33.
17 H. Gu, H. Zhang, C. Ma, X. Xu, Y. Wang, Z. Wang, R. Wei, H. Liu, C. Liu, Q. Shao, X. Mai and Z. Guo, *Carbon*, 2019, **142**, 131–140.
18 M. Park, H. Lee, J. U. Jang, J. H. Park, C. H. Kim, S. Y. Kim and J. Kim, *Compos. Sci. Technol.*, 2019, **177**, 96–102.
19 T. Fujigaya and N. Nakashima, *Sci. Technol. Adv. Mater.*, 2015, **16**, 4802–4822.
20 E. Koufakis, T. Manouras, S. H. Anastasiadis and M. Vamvakaki, *Langmuir*, 2020, **36**, 3482–3493.
21 L. Jian, L. Yan and S. Xin, *Chin. J. Catal.*, 2012, **33**, 891–897.
22 V. Skakalova, A. B. Kaiser, U. Dettlaff-Weglikowska, K. Hrncarikova and S. Roth, *J. Phys. Chem. B*, 2005, **109**, 7174–7181.
23 R. Wang, J. Sun, L. Gao and J. Zhang, *J. Mater. Chem.*, 2010, **20**, 6903–6909.
24 S. Qu, M. Li, L. Xie, X. Huang, J. Yang, N. Wang and S. Yang, *ACS Nano*, 2013, **7**, 4070–4081.
25 D. Zhang, M. G. Villarreal, E. Cabrera, A. Benatar, L. J. Lee and J. M. Castro, *Composites, Part B*, 2019, **159**, 327–335.

26 T. Zheng, G. Wang, N. Xu, C. Lu, Y. Qiao, D. Zhang and X. Wang, *Nanomaterials*, 2018, **8**, 969–973.
27 P. E. Lopes, F. van Hattum, C. M. C. Pereira, P. J. R. O. Novoa, S. Forero, F. Hepp and L. Pambaguian, *Compos. Struct.*, 2010, **92**, 1291–1298.
28 M. B. Jakubinek, B. Ashrafi, J. Guan, M. B. Johnson, M. A. White and B. Simard, *RSC Adv.*, 2014, **4**, 57564–57573.
29 Z. Spitalsky, G. Tsoukleri, D. Tasis, C. Krontiras, S. N. Georga and C. Galiotis, *Nanotechnology*, 2009, **20**, 1291–1298.
30 B. P. Singh, Prasanta, V. Choudhary, P. Saini, S. Pande, V. N. Singh and R. B. Mathur, *J. Nanopart. Res.*, 2013, **15**, 1554–1564.
31 G. Trakakis, D. Tasis, C. Aggelopoulos, J. Parthenios, C. Galiotis and K. Papagelis, *Compos. Sci. Technol.*, 2013, **77**, 52–59.
32 W. Lin, Q. Q. Shi, H. Chen and J. N. Wang, *Carbon*, 2019, **153**, 308–314.
33 T. Q. Tran, Z. Fan, P. Liu, S. M. Myint and H. M. Duong, *Carbon*, 2016, **99**, 407–415.